Dyes and Pigments 109 (2014) 169–174

Contents lists available at ScienceDirect

Dyes and Pigments

journal homepage: www.elsevier.com/locate/dyepig

Novel enantioselective fluorescent sensors for malate anion based on acridine

Qian Li [a], Kuoxi Xu [a, *], Pan Song [a], Yanpeng Dai [a], Li Yang [a], Xiaobin Pang [b, **]

[a] Institute of Fine Chemical and Engineering, College of Chemistry and Chemical Engineering, Henan University, Kaifeng, Henan 475004, PR China
[b] Institute of Pharmacy, Henan University, Kaifeng, Henan 475004, PR China

ARTICLE INFO

Article history:
Received 25 February 2014
Received in revised form
3 May 2014
Accepted 12 May 2014
Available online 21 May 2014

Keywords:
Enantioselective recognition
Fluorescent sensor
Malate anion
Fluorescence titration
Acridine
PET

ABSTRACT

The compounds **L-1** and **L-2** were synthesized and the interactions of all of the compounds with malate anion were studied by fluorescent titration and ^{1}H NMR experiments. The Sensors **L-1** and **L-2** were found to present good enantioselective fluorescent sensing ability to malate anion. The results indicated that sensors **L-1** and **L-2** were very promising to be used as fluorescent sensors in determining malate anion in CH_3CN.

1. Introduction

During the past two decades, considerable attention has been focused on the design of chiral substrates that can recognize and sense chiral anions selectively due to the important roles and potential applications anions play in environmental, biological and supramolecular sciences [1–5]. Among these chiral anions, malate anion (MA) plays significant role in pharmaceutics. *D*-Malate can only be found if the synthetic racemate is used as food additive. *L*-Malate is used in the treatment of light-damaged or dry skin, acne, and especially fibromyalgia when combined with magnesium. *L*-Malate is also used to treat atherosclerosis [6,7]. Therefore, the practical, rapid and accurate methods applied in enantioselective recognition of *D*- and *L*-malate are an important analytical agenda.

Up to now, many analytical methods such as nuclear magnetic resonance (NMR), high-performance liquid chromatography, circular dichroism have been developed for chiral anions determination, fluorescent sensors present many appealing advantages, including high sensitivity and selectivity, low cost, easy detection, and especially suitability as a diagnostic tool for biological concern [8–14]. To the best of our knowledge, few chiral fluorescent sensors have been reported up till now for the enantioselective recognition of MA in CH_3CN. In this paper, we reported the synthesis and enantioselective recognition of fluorescent MA sensors developing from acridine.

2. Experimental section

2.1. Materials

The reagents were used of commercial origin and were employed without further purification. Purifications by column chromatography were carried out over silica gel (230–400 mesh). The IR spectra were performed on a Nicolet 670 FT-IR spectrophotometer. ^{1}H NMR and ^{13}C NMR spectra were recorded on a Bruker AV-400 spectrometer. Mass spectra were determined by ESI recorded on an Esquire 3000 LC–MS mass instrument. Optical rotations were taken on a Perkin–Elmer Model 341 polarimeter. Elemental analyses were performed by the Vario Elemental CHSN-O microanalyzer. Fluorescence spectra were obtained with an F-7000 FL Spectrophotometer. The anions were used as their tetrabutylammonium salts. 4,5-Bis(bromomethyl)acridine was prepared according to the literature methods [15,16].

2.2. Syntheses

2.2.1. Syntheses of Boc-amino alcohol

$(Boc)_2O$ (2.10 g, 12 mmol) was added to a solution of amino alcohol (10 mmol) and diisopropylethylamine (DIPEA) (1.44 g,

* Corresponding author. Tel./fax: +86 371 23881589.
** Corresponding author.
E-mail addresses: xukx@henu.edu.cn, xkuox@163.com (K. Xu).

http://dx.doi.org/10.1016/j.dyepig.2014.05.017
0143-7208/

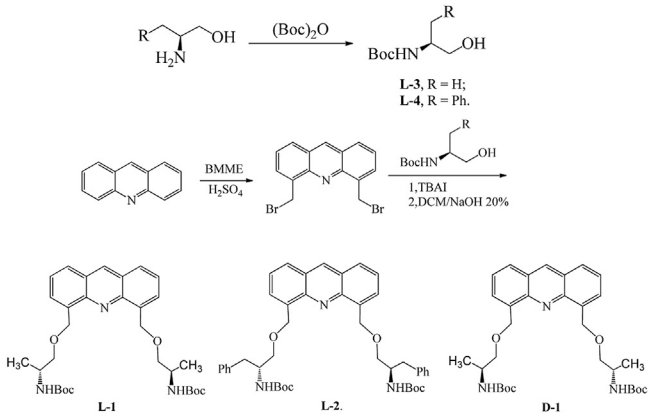

Scheme 1. Synthesis of compounds **L-1**, **D-1** and **L-2**.

12 mmol) in THF(40 mL) under N_2 protection at 0 °C. The mixture was stirred for 6 h at room temperature, then the solvent was removed under reduced pressure and the resulting residue was dissolved in 100 mL ethyl acetate. This solution was washed twice with 100 mL of water, once with 100 mL of saturated aqueous sodium chloride, dried over Na_2SO_4 and concentrated under reduced pressure to give product **L-3** or **L-4** as yellow oil.

L-3: 1.70 g, yield 97%; $[\alpha]_D^{20} = -8.4$ (*c* 0.05, $CHCl_3$); ^1H NMR($CDCl_3$): δ 4.71 (s, 1H), 3.69–3.60 (m, 1H), 3.57–3.42 (m, 2H), 2.21 (s, 1H), 1.36 (s, 9H), 1.12 (d, J = 6.4 Hz, 3H).

L-4: 2.38 g, yield 95%; $[\alpha]_D^{20} = -20.8$ (*c* 0.05, $CHCl_3$); ^1H NMR($CDCl_3$): δ 7.36–7.21 (m, 5H), 4.71 (s, 1H), 3.87 (s, 1H), 3.66–3.55 (m, 2H), 2.84 (d, J = 7.8 Hz, 2H), 2.23 (s, 1H), 1.41 (s, 9H).

2.2.2. *General procedure for the preparation of compounds **L-1**, **D-1** and **L-2***

To a solution of 4,5-bis(bromomethyl)acridine (0.37 g, 1.0 mmol) in dichloromethane (10 mL), 20% NaOH (10 mL), tetrabutylammonium iodide (0.81 g, 2.2 mmol) and *N*-Boc-amino alcohol (2.2 mmol) were added consecutively. The biphasic mixture was then stirred at room temperature for 15 h and monitored via TLC, after which it was poured into a separatory funnel over water and extracted with dichloromethane. The combined organic extracts were rinsed with brine, dried over anhydrous Na_2SO_4 and purified by means of flash chromatography over silica gel using petroleum ether: ethyl acetate (10:1) as eluent to obtain pure product **L-1**, **D-1** and **L-2** as yellow solid, respectively.

L-1: 0.23 g, m.p.: 132–133 °C, yield, 42.2%. $[\alpha]_D^{20} = -12.6$ (c = 0.20, $CHCl_3$); **D-1**: The preparation procedure the same as that of **L-1** with the use of R-N-Boc-amine alcohol as the materials. 0.24 g, m.p.:135–136 °C, yield, 42.4%, $[\alpha]_D^{20} = +12.2$ (c = 0.20, $CHCl_3$); ^1H NMR ($CDCl_3$) : δ 8.75 (s, 1H), 7.93(d, J = 8.4 Hz, 2H), 7.88(d, J = 7.6 Hz, 2H), 7.55(t, J = 7.6 Hz, 2H), 5.38(s, 4H), 4.89(s, 2H), 3.98(s, 2H), 3.76–3.68(m, 4H), 1.43 (s, 18H), 1.29(d, J = 6.8 Hz, 6H); ^{13}C NMR ($CDCl_3$): 155.49, 145.95, 136.84, 136.03, 127.40, 127.24, 125.56, 74.44, 69.49, 46.53, 28.45, 18.28, IR (KBr):3373, 1691, 1521, 1253, 1128, 758 cm^{-1}; HRMS *m/z*: calculated for $C_{31}H_{43}N_3O_6$, $[M+H]^+$ 554.3225, found 554.3229.

L-2: 0.37 g, m.p.: 141–142 °C, yield, 52.8%. $[\alpha]_D^{20} = -15.6$ (c = 0.20, $CHCl_3$); ^1H NMR ($CDCl_3$): δ 8.78 (s, 1H), 7.95(d, J = 8.4 Hz, 2H), 7.89(d, J = 6.8 Hz, 2H), 7.57(t, J = 7.6 Hz, 2H), 7.24–7.17(m, 10H), 5.32(d, J = 5.8 Hz, 4H), 5.03(s, 2H), 4.04(s, 2H), 3.66–3.40(m, 4H), 2.98(d, J = 4.0 Hz, 4H), 1.41 (s, 18H); ^{13}C NMR ($CDCl_3$): 155.44, 146.00, 138.35 136.84, 136.09 129.52, 128.39, 127.62, 126.30, 126.23, 125.61, 71.04, 69.46, 52.09, 51.98, 38.12, 38.09, 28.44; IR (KBr): 3365, 1689, 1522, 1390, 1365, 1249, 1170, 757, 700 cm^{-1}; HRMS *m/z*: calculated for $C_{43}H_{51}N_3O_6$, $[M+H]^+$ 706.3851, found 706.3856.

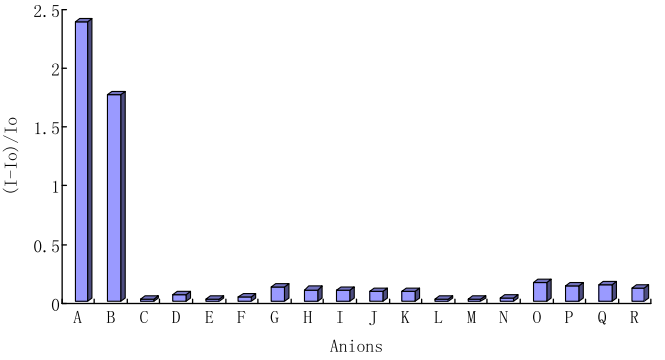

Fig. 1. Fluorescent spectra changes of sensor **L-1** (3.0×10^{-5} M) measured in CH_3CN upon the addition of 100 equivalent of various anions (λ_{ex} = 356 nm, λ_{em} = 423 nm). Fluorescent enhancement ($(I - I_0)/I_0$) of sensor **L-1** (3.0×10^{-5} M) at 423 nm upon the addition of different carboxylate anions (as tetrabutylammonium) in CH_3CN at 25 °C (100 equiv, 3.0×10^{-3} M). A = *D*-MA, B = *L*-MA, C = *L*-mandelic acid anion, D = *D*-mandelic acid anion, E = *L*-phenyl-lactic acid anion, F = *D*-phenyllactic acid anion, G = *L*-methoxyphenylacetic acid anion, H = *D*-methoxyphenylacetic acid anion, I = *L*tartaric acid anion, J = *D*-tartaric acid anion, K = *L*-dibenzoyltartaric acid anion, L = *D*-dibenzoyltartaric acid anion, M = *L*-phenylglycine anion, N = *D*-phenylglycine anion, O = *L*-phenylalanine anion, P = *D*-phenylalanine anion.

3. Results and discussion

3.1. Synthesis

The chiral fluorescence sensors **L-1** and **L-2** were efficiently synthesized by the reaction of intermediate *D*-N-Boc-amino alcohol **L-3** or **L-4** and 4,5-Bis(bromomethyl)acridine (Scheme 1). The preparation procedure of compound **D-1**, the enantiomers of **L-1**, was the same as that of **L-1** by starting with *D*-N-Boc-amino alcohol and 4,5-Bis(bromomethyl)acridine. The ^1H NMR spectra exhibited all the expected signals with the desired integral values and support the molecular structures. The structures of these compounds were characterized by IR, MS, ^1H NMR and ^{13}C NMR spectra. We chose these compounds to undertake the desired fluorescent recognition of MA for the following two reasons: on one hand, the oxygen atoms of the compounds could bind –OH of guest MA well through multiple hydrogen bonds. On the other hand, when the sensors interact with MA, their oxygen atoms were expected to turn on the fluorescence of the sensors by inhibiting the photoinduced-electron-transfer (PET) [17–19] of the oxygen atoms.

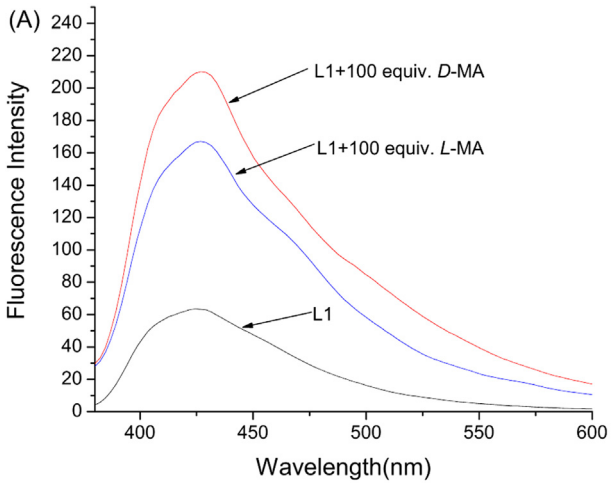

Fig. 2. Fluorescent spectra of **L-1** (3.0×10^{-5} M) with 100 equiv. of *D*- and *L*-MA in CH_3CN.

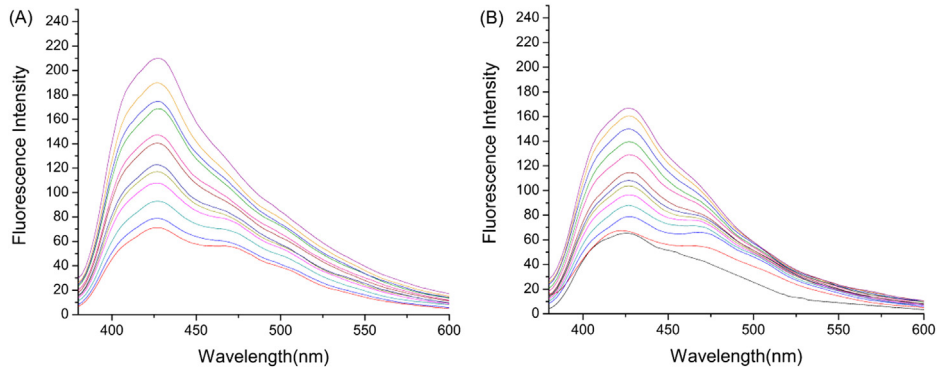

Fig. 3. (A) Fluorescent intensity changes of sensor **L-1** (3.0×10^{-5} M) with *D*-MA in CH_3CN. The *D*-MA equivalents are: 0 → 100. (B) The fluorescent intensity changes of sensor **L-1** with *L*-MA .The *L*-MA equivalents are: 0 → 100.

3.2. Fluorescence spectroscopic studies

Because there was almost no change on the UV–vis spectra of sensor **L-1** or **L-2** upon the addition of carboxylate anions, such as *D*- or *L*-phenylalanine, mandelate, methoxyphenylacetic acid, phenyl-lactic acid, tartaric acid, dibenzoyltartaric acid, MA (as tetrabutylammonium salts) in CH_3CN, even when the guests were excessive ([guest]/[**L-1** or **L-2**] = 100, see Supplementary Data Fig. s1). The properties of enantioselective recognition of sensor **L-1** or **L-2** were only investigated for *D*- or *L*-MA by the fluorescence spectra.

When the solution of sensor **L-1** was excited at 356 nm, it gave a characteristic emission spectrum with monomeric acridine maximum at ca 423 nm in CH_3CN. Binding behaviors of sensor **L-1** with different carboxylate anion in CH_3CN were investigated. Fig. 1 showed the changes of emission spectra of **L-1** (3.0×10^{-5} M) upon the addition of various carboxylate (see Supplementary Data, Fig. s2), only MA induced an increasing intensity. Other anions did not show any apparent spectral changes. These results indicated that MA could behave as a "turn-on" fluorescence sensor for selectively sensing MA over other investigated guests. Fig. 2 showed different fluorescent intensity changes when the same equivalent of *D*- or *L*-MA was added to sensor **L-1** in CH_3CN, respectively. These experiments demonstrated that sensor **L-1** had a highly enantioselective recognition ability towards the MA.

The binding constant (K_{ass}) of complexes of aforementioned chiral fluorescent sensor with MA was determined by means of titration fluorimetry. With the assumption of a 1:1 stoichiometry, the complexation of MA (G) with sensor (H) was expressed by Equation (1):

$$H + G \overset{K}{\rightleftharpoons} HG \quad (1)$$

Under the conditions employed, the association constant (K_{ass}) could be calculated by using Equation (2) from the Origin 7.5 software package [20,21]. *I* represented the fluorescence intensity,

Table 1
Association constants (K_{ass}) of sensor **L-1**, **D-1** and **L-2** with *D*- or *L*-MA at 25 °C.

Entry	Host	Guest[c]	*Ks*[M^{-1}][a,b]	$K_{(D)}/K_{(L)}$	*R*
1	L-1	*D*-MA	290 ± 2.1	3.92	0.9952
2	L-1	*L*-MA	74 ± 1.6		0.9985
3	D-1	*D*-MA	95 ± 3.2	0.45	0.9974
4	D-1	*L*-MA	198 ± 4.1		0.9959
5	L-2	*D*-MA	147 ± 2.8	3.13	0.9984
6	L-2	*L*-MA	47 ± 3.4		0.9993

[a] The data were calculated from the results of the fluorescent titrations in CH_3CN.
[b] All error values were obtained from nonlinear curve-fitting.
[c] MA were used as their tetrabutylammonium salts.

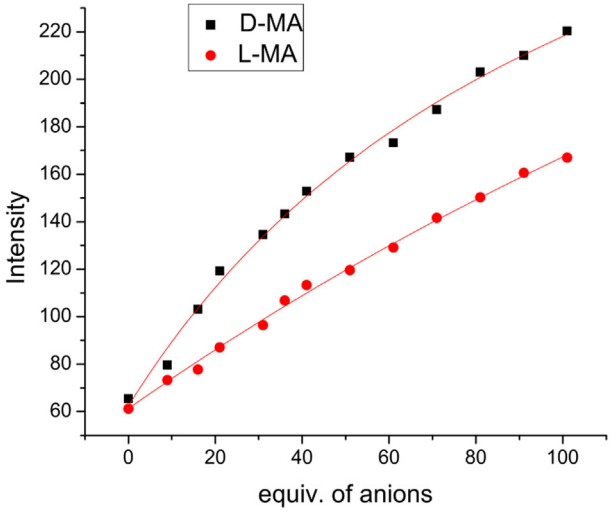

Fig. 4. Fluorescent intensity changes of sensor **L-1** at 423 nm with the addition of different amounts of *D*- or *L*-MA. The correlation coefficient (*R*) of the non-linear curve-fitting is 0.9952 and 0.9985, respectively.

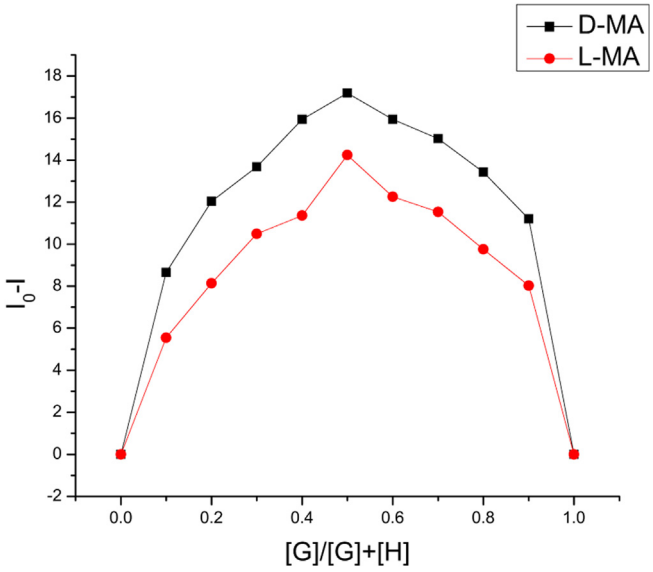

Fig. 5. Job plots of sensor **L-1** with *D*- and *L*-MA. The total concentration of the sensor **L-1** ([H]) and *D*- or *L*-MA ([G]) is (1.0×10^{-4} M) in CH_3CN. I_0: fluorescent intensity of sensor **L-1** and *I*: fluorescent intensity of sensor **L-1** in the presence of MA.

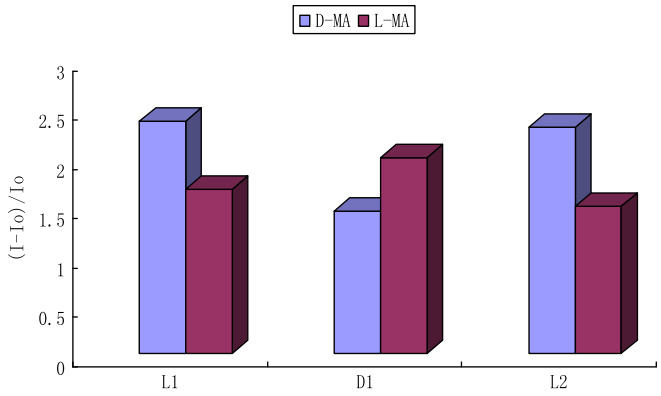

Fig. 6. Fluorescence spectral changes of sensors **L-1**, **D-1** and **L-2** (3.0×10^{-5} M) were measured upon the addition of 100 equiv. of *D*-or *L*-MA.

C_H and C_G were the sensor and anion concentrations respectively, and C_0 was the initial concentration of the sensor.

$$I = I_0 + (I_{lim} - I_0)\Big/2C_0\Big\{C_H + C_G + 1/K_{ass} - \Big[(C_H + C_G + 1/K_{ass})^2 - 4C_HC_G\Big]^{1/2}\Big\} \quad (2)$$

In order to know more about the interactions between **L-1** and *D*- or *L*-MA, fluorescent titration was carried out. When **L-1** was treated with *L*-MA, the emission gradually enhanced; while treated with *D*-MA under the same conditions, the emission of **L-1** larger enhanced (Fig. 3). The association constants (K_{ass}) and correlation coefficients (R) obtained by a nonlinear least squares analysis of I versus C_H and C_G were listed in Table 1. The results (the correlation coefficient R was over 0.99) of non-linear curve-fitting indicated that a 1:1 complex was formed between sensor **S-1** and *D*- or *L*-MA (Fig. 4).

The continuous variation methods were also employed to determine the stoichiometric ratio of sensor **L-1** with *D*- and *L*-MA. The total concentration of sensor **L-1** and *D*- or *L*-MA was constant (3.0×10^{-4} M) in CH_3CN, with a continuously variable molar fraction of the sensor ([H]/([H] + [G])). Fig. 5 showed the Job plots of sensor **L-1** with *D*- and *L*-MA. When the molar fraction of the sensor was 0.50, the fluorescent intensity reached the maximum, which demonstrated that sensor **L-1** formed a 1:1 complex with *D*- and *L*-MA, respectively [22,23].

In order to obtain better enantioselective fluorescent sensors, we used the large unit phenylalaninol as the started material to replace alaninol to get compound **L-2**. The enantioselectivities of **L-2** towards MA were compared with that of **L-1** towards MA. When compound **L-2** was treated with *D*-MA under the same conditions, the emission gradually enhanced; while treated with *L*-MA, the emission of sensor **L-2** lesser enhanced (Figs. s3 and s4), which gave *Ka*(*D*)/*Ka*(*L*) 3.13 for MA (Fig. 6, Table 1). The fluorescent sensor **L-2** was less enantioselective towards MA than sensor **L-1**. The increasing of satiric bulk maybe caused the obstacle in recognizing the fluorescent sensors towards MA.

The enantioselective fluorescent recognition of MA by **L-1** could be confirmed by using sensor **D-1**, which gave the expected mirror image responses for the enantiomers of MA (Figs. s5 and s6), that was, the enantiomer of *L*-MA increased the fluorescence of **L-1** more efficiently than the *D*-MA.

The chiral fluorescent sensors **L-1** and **L-2** containing nitrogen were synthesized by simple steps, and their enantioselective recognition abilities towards MA were evaluated by the fluorescence spectra. Probably NH group of the sensors interacted with carboxylates of MA due to enantioselective recognition. To our knowledge, this was the first reported fluorescent sensor for the enantioselective recognition of MA in CH_3CN. Sensor **L-1** exhibited the highest association constants and the best enantioselective recognition towards MA. The sensors' structure-complementary, steric effect with MA and multiple hydrogen bonding should be responsible for the enantioselective recognition. Sensitive fluorescent response revealed that sensor **L-1** could be used as a fluorescent sensor for MA in CH_3CN.

3.3. ^1H NMR studies

^1H NMR experiments were undertaken to assess the enantioselective recognition properties between sensor and *D*- or *L*-MA because it could directly provide structural and dynamic

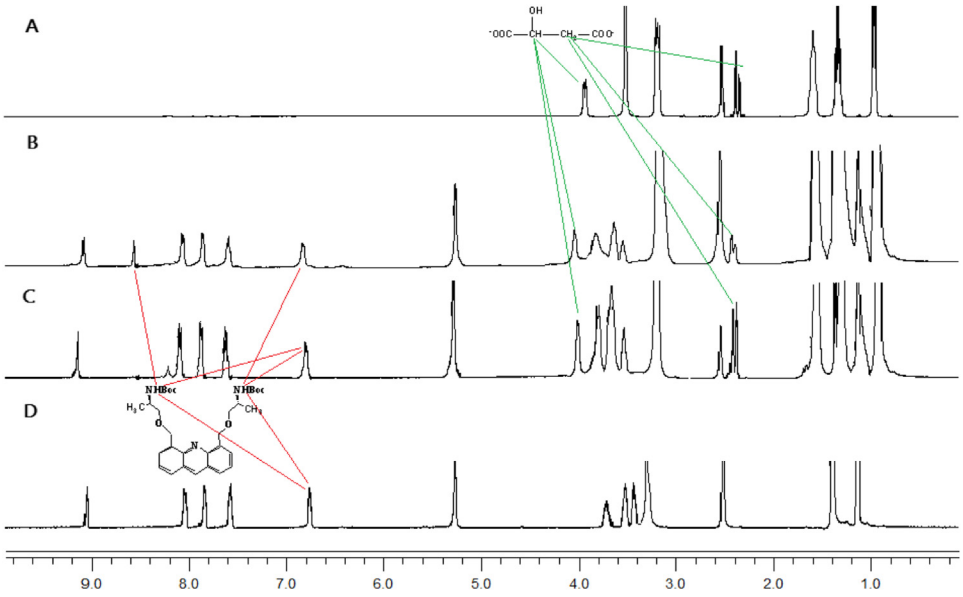

Fig. 7. ^1H NMR spectra (400 MHz, DMSO-d_6 25 °C) of **L-1** and MA complex at ([**L-1**] = [guest] = 4.0 nM in DMSO-d6 at 400 MHz). (A) Racemic MA; (B) sensor **L-1** + *D*-MA; (C) sensor **L-1** + *L*-MA; (D) sensor **L-1**.

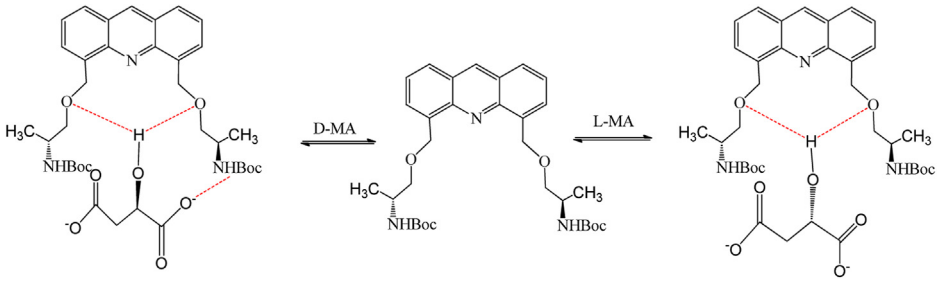

Fig. 8. Modes of the proposed 1:1 complexation of sensor **L-1** with the *D*- and *L*-MA.

information [24,25]. Studies on the enantioselective recognition were carried out on a 400 MHz NMR spectrometer using **L-1** as chiral solvating agents. Fig. 7 showed the spectra of **L-1** in DMSO-d_6 solution in the absence and in the presence of 1.0 equiv. *D*- or *L*-MA (Fig. 7B, C). Notice that in the presence of *D*-MA of **L-1** the chiral C**H** proton of free MA were downshift to 4.09 ppm ($\Delta\delta$ = 0.13 ppm, Fig. 7B), but the C**H** proton of MA show resonance at 4.04 ppm in the presence of **L-1** (Fig. 7C). The interaction of sensor **L-1** with the *D*-MA showed that the CH proton has a larger downfield shift than the chiral C**H** proton of the *L*-enantiomer. The signal of the amide (NH) group linked to the Boc moiety of **L-1** was also shifted partly downfield from δ 6.78 to 8.54 ($\Delta\delta$ = 1.76 ppm, Fig. 7B) in the presence of *D*-MA, this resonance in two amide group reflected different action on the sensor, maybe since only one of them could interact directly with the guest MA (Fig. 7B, C), whereas the amide groups exhibited nearly no change (Fig. 7C) in the presence *L*-MA. Notice also that the methylene protons next to acridine at 5.27 ppm and the other methylene protons next to chiral center at 3.79 and 3.60 ppm of the free **L-1**, once the guest MA was added, the methylene protons resonances had different downshifted (Fig. 7B, C, D) indicated that the methylene protons next to chiral center of **L-1** showed a larger influence with MA than another methylene.

Therefore, as the proposed modes showed in Fig. 8, the hydroxy group of *D*-MA may form hydrogen bonds with the oxygen atoms of **L-1**, according to the orientation of the carboxylate anion in MA combined with the NH group.

The above results illustrated that the nature of the receptor, multiple hydrogen-bonding interactions, and complementary stereogenic center interactions should be responsible for the enantioselective recognition of MA [26,27].

4. Conclusion

In conclusion, we had been demonstrated that with the introduction of *N*-Boc protected amine alcohol to the acridine, the easily accessible acridine-based chiral fluorescence sensor **L-1** and **L-2** were excellent enantioselective fluorescent sensor for MA. To our knowledge, it was the first excellent enantioselective fluorescent sensor for malate anion. Such sensors were potentially useful for throughput chiral assays and chiral catalyst screening.

Acknowledgments

We thank the National Natural Science Foundation of China (Grant No. 81273652), Technological Project of Henan Province (132300410055, 132102210388) and the Education Department of Henan Province of China (14A150050) for financial support.

Appendix A. Supplementary data

Supplementary data related to this article can be found at http://dx.doi.org/10.1016/j.dyepig.2014.05.017.

References

[1] Kim SK, Lee DH, Hong J, Yoon J. Chemosensors for pyrophosphate. Acc Chem Res 2009;42:23–31.
[2] Pu L. Fluorescence of organic molecules in chiral recognition. Chem Rev 2004;104:1687–716.
[3] dos Santos CMG, Harte AJ, Quinn SJ, Gunnlaugsson T. Recent developments in the field of supramolecular lanthanide luminescent sensors and self-assemblies. Coord Chem Rev 2008;252:2512–27.
[4] Renuga D, Udhayakumari D, Suganya S, Velmathi S. Novel thiophene based colorimetric and fluorescent receptor for selective recognition of fluoride ions. Tetrahedron Lett 2012;53:5068–70.
[5] KXi Xu, Kong HJ, Li P, Yang L, Zhang JL, Wang CJ. Acridine-based enantioselective fluorescent sensors for the malate anion in water. New J Chem 2014;38:1004–10.
[6] Bergmeyer HU. Methods of enzymatic analysis. In Metabolites 2, vol. VII. Germany: VCH; 1985.
[7] Ziyatdinov A, Fernández Diaze E, Chaudryc A, Marco S, Persaud K, Pereraa A. A software tool for large-scale synthetic experiments based on polymeric sensor arrays. Sens Actuators B 2013;18:596–604.
[8] Li ZB, Lin J, Sabat M, Hyacinth M, Pu L. Enantioselective fluorescent recognition of chiral acids by cyclohexane-1,2-diamine-based bisbinaphthyl molecules. J Org Chem 2007;72:4905–16.
[9] Qing GY, Sun TL, Chen ZH, Yang X, Wu XJ, He YB. 'Naked-eye' enantioselective chemosensors for N-protected amino acid anions bearing thiourea units. Chirality 2009;21:363–73.
[10] Su XY, Luo K, Xiang QX, Lan JB, Xie RG. Enantioselective recognitions of chiral molecular tweezers containing imidazoliums for amino acids. Chirality 2009;21:539–46.
[11] Liu HL, Zhao QL, Hou XL, Pu L. Clarification of a misconception in the BINOL-based fluorescent sensors: synthesis and study of major-groove BINOL-amino alcohols. Chem Commun 2011;47:3646–8.
[12] Chi L, Zhao JZ, James TD. Chiral mono boronic acid as fluorescent enantioselective sensor for mono a-hydroxyl carboxylic acids. J Org Chem 2008;73:4684–7.
[13] Williams AA, Fakayode SO, Lowry M, Warner IM. A versatile chiral selector for determination of enantiomeric composition of fluorescent and nonfluorescent chiral molecules using steady-state fluorescence spectroscopy. Chirality 2009;21:305–15.
[14] Williams AA, Fakayode SO, Alptrk OC, Jones M, Lowry M, Strongin RM, et al. Determination of enantiomeric compositions of analytes using novel fluorescent chiral molecular micelles and steady state fluorescence measurements. J Fluoresc 2008;18:285–96.
[15] Chiron J, Galy JP. Reactivity of the acridine ring: one-pot regioselective single and double bromomethylation of acridine and some derivatives. Synlett 2003;15:2349–50.
[16] Ebner C, Pfaltz A. Chiral dihydrobenzo[1,4]oxazines as catalysts for the asymmetric transfer-hydrogenation of α, β-unsaturated aldehydes. Tetrahedron 2011;67:10287–90.
[17] Liu HL, Peng Q, Wu YD, Chen D, Hou XL, Sabat M, et al. Highly enantioselective recognition of structurally diverse α-hydroxycarboxylic acids using a fluorescent sensor. Angew Chem Int Ed 2010;49:602–6.
[18] Xu KX, Jiao SY, Yao WY, Kong HJ, Zhang JL, Wang CJ. Syntheses and highly enantioselective fluorescent recognition of α-hydroxyl/amino carboxylic acid anions in protic solutions. Sens Actuators B 2013;177:384–9.
[19] Xu KX, Yang LR, Wang YX, Zhao J, Wang CJ. Synthesis and enantioselective fluorescent sensors for amino acid derivatives based on BINOL. Supramol Chem 2010;22:563–70.
[20] Xu KX, Cheng PF, Zhao J, Wang CJ. Enantioselective fluorescent sensors for amino acid derivatives based on BINOL bearing S-tryptophan unit: synthesis and chiral recognition. J Fluoresc 2011;21:991–1000.
[21] Valeur B, Pouget J, Bourson J, Kaschke M, Ernsting NP. Tuning of photoinduced energy transfer in a bichromophoric coumarin supermolecule by cation binding. J Phys Chem 1992;96:6545–9.
[22] Li Z, Zhou Y, Yin K, Yu Z, Li Y, Ren J. A new fluorescence "turn-on" type chemosensor for Fe^{3+} based on naphthalimide and coumarin. Dyes Pigment 2014;105:7–11.

[23] Schneider HJ, Yatsimirsky AK. Principles and methods in supramolecular chemistry. New York: John Wiley & Sons; 2000.
[24] Pirkle WH, Pochapsky TC. Considerations of chiral recognition relevant to the liquid chromatography separation of enantiomers. Chem Rev 1989;89:347–62.
[25] Xu KX, Wu XJ, He YB, Liu SY, Qing GY, Meng LZ. Synthesis and chiral recognition of novel chiral fluorescence receptors bearing 9-anthryl moieties. Tetrahedron Asymmetry 2005;16:833–9.
[26] Xu KX, Jiao SY, Yao WY, Xie E, Tang BW, Wang CJ. Syntheses and highly enantioselective fluorescent recognition of a-aminocarboxylic acid anions using chiral oxacalix[2]arene[2]bisbinaphthes. Chirality 2012;24:646–51.
[27] Xu KX, Kong HJ, Zu FL, Yang L, Wang CJ. A pair of chiral fluorescent sensors for enantioselective recognition of mandelate in water. Spectrochim Acta Part A 2014;118:811–5.